# Circadian Vesicle Capture Prepares Clock Neuron Synapses for Daily Phase-Delayed Neuropeptide Release

Markus K. Klose[1], Junghun Kim[1], Brigitte F. Schmidt[2] and Edwin S. Levitan[1]*

[1]Department of Pharmacology and Chemical Biology, University of Pittsburgh, Pittsburgh, PA 15261, USA

[2]Department of Chemistry, Carnegie Mellon University, Pittsburgh, PA, 15213, USA

*Corresponding author: elevitan@pitt.edu

Short title: Rhythmic vesicle capture in clock neurons

Key words: neuropeptide vesicle capture, axonal transport, clock neurons, fluorogen-activating protein, DCV release, *Drosophila*

18 pages

4 Figures

*The authors declare no competing interests.*

ABSTRACT

***Drosophila*** **sLNv clock neurons release the neuropeptide PDF to control circadian rhythms. Strikingly, PDF content in sLNv terminals is rhythmic with a peak in the morning hours prior to the onset of activity-dependent release. Because synaptic PDF accumulation, rather than synaptic release, aligns with the late-night elevations in both sLNv neuron excitability and $Ca^{2+}$, we explored the dependence of presynaptic neuropeptide accumulation on neuropeptide vesicle transport, electrical activity and the circadian clock. Live imaging reveals that anterograde axonal transport is constant throughout the day and capture of circulating neuropeptide vesicles rhythmically boosts presynaptic neuropeptide content hours prior to release. The late-night surge in vesicle capture, like release, requires electrical activity and results in a large releasable pool of presynaptic vesicles to support the later burst of neuropeptide release. The circadian clock is also required suggesting that it controls the switch from vesicle capture to exocytosis, which are normally coupled activity-dependent processes. This toggling of activity transduction maximizes rhythmic synaptic neuropeptide release needed for robust circadian behavior and resolves the previously puzzling delay in timing of synaptic neuropeptide release relative to changes in sLNv clock neuron physiology.**

## Introduction

*Drosophila* sLNv neurons release the neuropeptide Pigment Dispersing Factor (PDF) to synchronize molecular rhythms of individual neurons in the clock circuit to maintain daily rhythms in motor activity (Yoshii *et al.*, 2009; Ahmad *et al.*, 2021). Interestingly, PDF content in these neurons is rhythmic (Park *et al.*, 2000) with a drop in presynaptic PDF in the late morning caused by activity-dependent dense-core vesicle (DCV) exocytosis (Klose *et al.*, 2021). Furthermore, rhythmic exocytosis is preceded by an hours long surge in terminal neuropeptide content (Park *et al.*, 2000; Klose *et al.*, 2021), which is advantageous because release scales with presynaptic neuropeptide stores (Bulgari et al., 2014; Cavolo et al., 2016). Daily increases in presynaptic PDF stores are not driven by PDF gene expression (Park *et al.*, 2000). Instead, it was hypothesized that transport from the soma is controlled by bursting electrical activity to regulate sLNv terminal neuropeptide content (Fernandez-Chiappe *et al.*, 2021). However, because anterograde axonal transport of DCVs in sLNv neurons has not been examined directly, the mechanism underlying the rhythmic increase in presynaptic neuropeptide stores in these clock neurons is unknown.

Recently, Klose, *et al.* (2021) showed that the DCV marker Dilp2-GFP (GFP-tagged *Drosophila* proinsulin-like peptide 2) (Wong *et al*., 2012) recapitulates rhythmic PDF content changes in sLNv terminals including the late-night/early morning increase in neuropeptide content and the subsequent drop hours later. Furthermore, the same study determined with FAP (fluorogen-activating protein) imaging that the timing of daily synaptic neuropeptide release coincides with the drop in synaptic PDF content. Interestingly, rhythmic release by sLNv clock neurons (Klose *et al.*, 2021) is brief and

phase delayed compared to changes in sLNv neuron excitability and intracellular calcium concentration ($[Ca^{2+}]_i$) (Cao and Nitabach, 2008; Liang *et al.*, 2016). In fact, contrary to the common use of surrogates to deduce synaptic transmission, the elevation of presynaptic neuropeptide content in sLNv terminals, rather than synaptic release, coincides with the daily increases in both electrical excitability and $[Ca^{2+}]_i$. The latter observation raises the question of whether activity-dependent capture of circulating DCVs (Shakiryanova *et al.*, 2006; Wong *et al.*, 2012) contributes to the early morning elevation of presynaptic PDF.

Here, Dilp2-GFP imaging is first used to determine how DCV transport in sLNv axons produces the late night/early morning increase in presynaptic neuropeptide in preparation for release hours later. These experiments do not support a role for increased anterograde axonal transport as previously proposed, but instead show that a rhythmic increase in DCV capture causes accumulation of presynaptic neuropeptide hours before daily bouts of release. Follow-up experiments explore how this capture relates to concurrent morphological changes (Fernandez *et al.*, 2008) and changes in locomotor behavior prior to sunrise (i.e., morning anticipation), each of which depends on the PDF receptor (PDFR) (Hyun *et al.*, 2005; Herrero *et al.*, 2020), electrical activity and the circadian clock.

## Results and Discussion

To test the hypothesis that increased delivery of DCVs to sLNv terminals upregulates presynaptic neuropeptide content in the late night/early morning, axonal transport of GFP-labeled DCVs was imaged in brain explants isolated at different times

of the day from PDF>Dilp2-GFP (w; UAS-Dilp2-GFP; PDF-GAL4) flies. Initially, the ratio of anterograde DCV flux to retrograde DCV flux (A/R) was measured from kymographs (Fig. 1A,B). These experiments showed that the flux ratio changed ($P < 0.001$, one-way ANOVA) with a peak late at night (i.e., at ZT23) (Fig. 1B,C), a time when *Drosophila* display morning anticipation and PDF is accumulating in sLNv terminals in preparation for subsequent release. Thus, in the hours prior to release there is a net increase in axonal transport of DCVs to sLNv terminals to upregulate presynaptic neuropeptide content.

Anterograde and retrograde DCV transport were then examined individually to determine which component of the flux ratio changed, the numerator (A) or the denominator (R). Analysis of axonal transport showed that anterograde DCV flux (A) was constant at all times tested (Fig. 2A), thus ruling out rhythmic changes in the ratio being driven by anterograde axonal transport from the soma. Rather, retrograde axonal DCV flux (R) cycled ($P < 0.01$, one-way ANOVA) with a minimum in the late night at ZT23 (Fig. 2B). This drop in retrograde flux cannot be explained by exocytosis-induced DCV depletion since the drop precedes daily synaptic neuropeptide release by several hours (Klose *et al.*, 2021). Furthermore, the decrease in retrograde flux occurred without altering the velocity of retrograde DCVs (Fig. 2C), thus excluding a slowing of the retrograde transport motors. Therefore, the observed reduction in retrograde flux is indicative of increased synaptic capture of circulating DCVs (Shakiryanova *et al.*, 2006; Wong *et al.*, 2012), which causes presynaptic neuropeptide content to increase.

Capture of circulating DCVs at synaptic boutons occurs through independent mechanisms that operate either constitutively or in response to activity (Shakiryanova *et*

*al.*, 2006; Wong *et al.*, 2012; Cavolo *et al.*, 2016). Activity-dependent capture was discovered at the neuromuscular junction based on a drop in retrograde axonal DCV transport (Shakiryanova *et al.*, 2006). Furthermore, silencing electrical activity in PDF releasing neurons by expression of the Kir2.1 channel eliminates circadian free-running locomotor behavior and daily rhythmic changes in PDF in sLNv terminals (Nitabach *et al.*, 2002; Depetris-Chauvin *et al.*, 2011). Therefore, we tested the hypothesis that activity-dependent vesicle capture produces the rhythmic increase in presynaptic PDF. Specifically, this hypothesis predicts that Kir2.1-induced silencing should eliminate the difference in DCV capture in sLNv neurons that is evident between ZT23 and ZT3, possibly with a compensatory change in baseline constitutive capture. In accordance with the hypothesis, cell-specific expression of Kir2.1 (see **Materials and methods**) eliminated the change in A/R ratio between the two time points (Fig. 3A). Thus, the daily change in vesicle capture depends on electrical activity.

Rhythmic changes in presynaptic neuropeptide content (Park *et al.*, 2000) overlap with morphological plasticity in the sLNv axonal arbor (Fernandez *et al.*, 2008). To probe whether presynaptic DCV capture and axonal morphology are linked, DCV axonal transport was studied in a PDF receptor (PDFR) null mutant (*han*), which prevents daily changes in terminal morphology while preserving rhythmic changes in PDF (Herrero *et al.*, 2020). In PDFR null animals the daily rhythmic changes in axonal flux ratio persisted (Fig. 3B). Therefore, the daily rhythm in DCV capture occurs independently of PDFR expression and the accompanying morphological plasticity it drives.

The PDFR null mutant also abolishes morning anticipation (Hyun *et al.*, 2005).

Because rhythmic capture occurs concurrently with this clock-dependent increase in locomotor behavior but persists when it is disrupted by the PDFR null mutation, we considered whether capture depends on the circadian clock. If capture is independent of the circadian clock, rhythmic capture would likely be driven through environmental cues, namely daily changes in light levels, and thus would be disrupted after shifting to constant conditions. However, after shifting to constant darkness (DD) capture remained different between CT23 and CT3 (Fig. 3C, CON). To further test for a role of the circadian clock, we examined the effect of a null mutation in the *period* gene ($per^{01}$) under DD conditions, which disrupts circadian rhythms. Consistent with the loss of oscillation in synaptic PDF content with this mutant (Park *et al.*, 2000), the difference in capture under DD conditions was disrupted in two lines of $per^{01}$ animals (Fig. 3C, 80928 and 80917). Therefore, rhythmic DCV capture in sLNv terminals depends on the circadian clock.

The consistent results for sLNv terminal PDF and neuropeptide vesicle flux in Kir2.1, *han* and $per^{01}$ experiments support the conclusion that vesicle capture underlies rhythmic presynaptic neuropeptide levels. However, the timing disparity in the daily rhythm peaks of synaptic DCV capture (ZT23, Figs. 1 and 2) and exocytosis (ZT3, Klose *et al.*, 2021) at sLNv terminals is surprising for two reasons. First, synaptic release is usually triggered rapidly and directly by activity, but synaptic DCV exocytosis by sLNv neurons (Klose *et al.*, 2021) peaks hours after sLNv neuron electrical excitability and $[Ca^{2+}]_i$ are elevated (Cao and Nitabach, 2008; Liang *et al.*, 2016). Second, at the neuromuscular junction activity-evoked DCV exocytosis and capture occur in rapid succession (Shakiryanova *et al.*, 2006), while the daily peak in DCV

capture in sLNv terminals precedes rhythmic activity-dependent synaptic neuropeptide release by several hours. Thus, activity-dependent DCV exocytosis is unexpectedly phase-delayed relative to $[Ca^{2+}]_i$, excitability and activity-dependent DCV capture increases.

A potential explanation for the delay in release is that DCVs in sLNv terminals are not yet releasable when capture peaks and only become competent for release later in the morning (i.e., the releasable pool is initially small because DCVs must be slowly primed to respond to activity). To test this hypothesis, the DCV exocytosis response to supraphysiological $K^+$-induced depolarization was measured by FAP imaging (Klose *et al.*, 2021) at ZT1, a time point when neuropeptide stores have already expanded, but daily exocytosis has not yet been initiated. Strikingly, exocytosis in response to depolarization is robust at ZT1 (Fig. 4, Hi K+). Furthermore, the release evoked by depolarization at ZT1 is comparable to peak endogenous release at ZT3 (Klose et al., 2021), suggesting that endogenous rhythmic release depletes the releasable pool. To relate release to the total presynaptic pool, a membrane permeant fluorogen (MGnBu, Perkins *et al.*, 2018) was applied to label presynaptic Dilp2-FAP. This showed that the releasable pool was about half of the total neuropeptide pool in terminals (Fig. 4, MGnBu). Thus, at ZT1 there is a large pool of release-competent DCVs in sLNv terminals. This shows that the phase delay in exocytosis is not due to a change in vesicle releasability. Rather, the data imply that a toggle controlled by the circadian clock switches activity from inducing capture to inducing release. We suggest that, because activity-dependent capture is mediated by kinases (Wong *et al.*, 2009; Bharat *et al.*, 2017) and exocytosis is also subject to physiological regulation, circadian

signaling sets the time of day when activity induces either vesicle capture or exocytosis. Alternatively, the clock might influence expression of proteins involved in capture and/or release such as a synaptagmin or complexin (Bharat *et al.*, 2017; Luo *et al.*, 2018; Ma *et al.*, 2021). Regardless of the underlying mechanism, the toggling of the effects of activity resolves why the timing of DCV exocytosis in sLNv clock neurons does not align with elevations in electrical activity and $[Ca^{2+}]_i$, which are typically assumed to be indicative of synaptic release. Furthermore, the toggling from DCV capture to exocytosis during a long epoch of electrical activity ensures that the burst of rhythmic synaptic neuropeptide release by sLNv clock neurons is efficient and maximized.

**Materials and methods**

*Imaging*: Flies were entrained for at least for 72 hours in a 12 hour light: 12 hour dark (LD) schedule before dissection of 4-9 day old males to generate brain explants. Dissections during the dark phase were performed under a red light. Adult flies were immobilized with $CO_2$ gas and brains were dissected in 0 $Ca^{2+}$ HL3 saline solution (70 mM NaCl, 5 mM KCl, 20 mM $MgCl_2$*$6H_2O$, 115 mM Sucrose, 5 mM Trehalose, 5 mM Hepes, and 10 mM $NaHCO_3$, pH 7.3) and then put into polylysine-coated plastic dishes containing HL3 with 2 mM $Ca^{2+}$ for imaging (Klose et al., 2016). For DCV flux two axonal regions in the dorsal protocerebrum were imaged in each hemisphere of the brain on an upright Olympus microscope equipped with a 60× 1.1 NA dipping water immersion objective, a Yokogawa spinning disk confocal head, a 488 nm laser for GFP illumination, and a Teledyne Photometrics sCMOS camera. Time-lapse experiments entailed acquiring 180 images with 150 ms exposure times at 3 Hz. From these movies,

regions where dorsally projecting axons defasciculated from bundles were used for generating kymographs with the Kymograph plugin of Imagej. FAP imaging experiments were performed as previously described (Klose *et al.*, 2021). In the current experiments, a recombinant with UAS-Dilp2-GFP and UAS-Dilp2-FAP was used so that GFP could be used for focusing before application of the fluorogens MG-Tcarb or MGnBu. Analysis of brightness was done in Imagej or Fiji. Statistical analysis was performed with Graphpad Prism software.

*Fly lines*: A plasmid for UAS-Kir2.1 without a GFP tag provided by Sean Sweeney (University of York) was used by Bestgene Inc. to generate transgenic flies with an insertion in chromosome III. All flies used the PDF-Gal4 promoter on the third chromosome (provided by Paul Taghert, Washington University in St. Louis). The PDF-Gal4 drives expression in the two subsets of clock neuron that express PDF neuropeptide, the small ventrolateral (sLNv) neurons and large ventrolateral (lLNv) neurons. UAS-Dilp2-GFP and UAS-Dilp2-FAP were reported previously (Wong *et al.*, 2012 and Bulgari *et al.*, 2019, respectively). Finally, other lines were from the Bloomington *Drosophila* stock center including *Bl#* 33068 (*han*), *Bl#* 35785, UAS-mCherry RNAi and the $per^{01}$ lines *Bl#* 80928 and 80917.

**Funding**

This research was supported by National Institutes of Health grant R01NS032385 to ESL.

**Acknowledgements**

We thank Sean Sweeney (University of York) for providing the UAS-Kir2.1 plasmid and Paul Taghert (Washington University in St. Louis) for the PDF-Gal4 (III) flies. We are also thankful for suggestions from Marcel Bruchez (Carnegie Mellon University, deceased) and for comments on the manuscript from David Deitcher (Cornell University).

## References

Ahmad M, Li W, Top D. Integration of Circadian Clock Information in the Drosophila Circadian Neuronal Network. J Biol Rhythms. 2021;36(3):203-220.

Bharat V, Siebrecht M, Burk K, Ahmed S, Reissner C, Kohansal-Nodehi M, Steubler V, Zweckstetter M, Ting JT, Dean C. Capture of Dense Core Vesicles at Synapses by JNK-Dependent Phosphorylation of Synaptotagmin-4. Cell Rep. 2017;21(8):2118-2133.

Bulgari D, Zhou C, Hewes RS, Deitcher DL, Levitan ES. Vesicle capture, not delivery, scales up neuropeptide storage in neuroendocrine terminals. Proc Natl Acad Sci U S A. 2014;111(9):3597-601.

Cao G, Nitabach MN. Circadian control of membrane excitability in Drosophila melanogaster lateral ventral clock neurons.J Neurosci. 2008;28(25):6493-501.

Cavolo SL, Bulgari D, Deitcher DL, Levitan ES. Activity Induces Fmr1-Sensitive Synaptic Capture of Anterograde Circulating Neuropeptide Vesicles. J Neurosci. 2016;36(46):11781-11787.

Depetris-Chauvin A, Berni J, Aranovich EJ, Muraro NI, Beckwith EJ, Ceriani MF. Adult-specific electrical silencing of pacemaker neurons uncouples molecular clock from circadian outputs. Curr Biol. 2011;21(21):1783-93.

Fernández MP, Berni J, Ceriani MF. Circadian remodeling of neuronal circuits involved in rhythmic behavior. PLoS Biol. 2008;6(3):e69.

Fernandez-Chiappe F, Frenkel L, Colque CC, Ricciuti A, Hahm B, Cerredo K, Muraro NI, Ceriani MF. High-Frequency Neuronal Bursting is Essential for Circadian and Sleep Behaviors in Drosophila. J Neurosci. 2021;41(4):689-710.

Herrero A, Yoshii T, Ispizua JI, Colque C, Veenstra JA, Muraro NI, Ceriani MF. Coupling Neuropeptide Levels to Structural Plasticity in Drosophila Clock Neurons. Curr Biol. 2020;30(16):3154-3166.e4.

Hyun S, *et al.* Drosophila GPCR Han is a receptor for the circadian clock neuropeptide PDF. Neuron 2005; 48(2):267-278.

Klose MK, Bruchez MP, Deitcher DL, Levitan ES. Temporally and spatially partitioned neuropeptide release from individual clock neurons. Proc Natl Acad Sci U S A. 2021;118(17):e2101818118.

Klose MK, Duvall L, Li W, Liang X, Ren C, Steinbach J, Taghert P. Functional PDF Signaling in the Drosophila Circadian Neural Circuit Is Gated by Ral A-Dependent Modulation. Neuron. 2016;90(4):781-794.

Liang X, Holy TE, Taghert PH. Synchronous *Drosophila* circadian pacemakers display

nonsynchronous $Ca^{2+}$ rhythms *in vivo*. Science. 2016; 351(6276):976-81.

Luo W, *et al.* NonA and CPX link the circadian clockwork to locomotor activity in *Drosophila*. Neuron. 2018;99(4):768-780.e3.

Ma D, *et al.* A transcriptomic taxonomy of Drosophila circadian neurons around the clock. Elife. 2021; 10:e63056.

Nitabach MN, Blau J, Holmes TC. Electrical silencing of Drosophila pacemaker neurons stops the free-running circadian clock. Cell. 2002;109(4):485-95.

Park JH, Helfrich-Förster C, Lee G, Liu L, Rosbash M, Hall JC. Differential regulation of circadian pacemaker output by separate clock genes in Drosophila. Proc Natl Acad Sci U S A. 2000;97(7):3608-13.

Perkins LA, Fisher GW, Naganbabu M, Schmidt BF, Mun, F, Bruchez MP. High-content surface and total expression siRNA kinase library screen with vx-809 treatment reveals kinase targets that enhance F508del-CFTR rescue. Mol Pharm 2018; 5(3):759-767.

Shakiryanova D, Tully A, Levitan ES. Nat Neurosci. Activity-dependent synaptic capture of transiting peptidergic vesicles. 2006;9(7):896-900.

Wong MY, Shakiryanova D, Levitan ES. Presynaptic ryanodine receptor-CamKII

signaling is required for activity-dependent capture of transiting vesicles. J Mol Neurosci. 2009;37(2):146-50.

Wong MY, Zhou C, Shakiryanova D, Lloyd TE, Deitcher DL, Levitan ES. Neuropeptide delivery to synapses by long-range vesicle circulation and sporadic capture. Cell. 2012;148(5):1029-38.

Yoshii T, Wülbeck C, Sehadova H, Veleri S, Bichler D, Stanewsky R, Helfrich-Förster C. The neuropeptide pigment-dispersing factor adjusts period and phase of Drosophila's clock. J Neurosci. 2009;29(8):2597-610.

## Legends

**Figure 1. Dense-core vesicle flux in sLNv nerve terminal projections.**

Ai. sLNv projections containing DCVs filled with Dilp2-GFP at t=0.33 seconds of recording. White box reveals region of interest (ROI) for analysis. Aii. DCVs at t = 0, 0.33, 0.66, and 1.0 seconds (red arrow indicates anterograde (AR) transport and blue arrow indicates retrograde (RE) transport, scale bar = 1 μm). Aiii. Kymograph of ROI (red arrow anterograde, blue arrow retrograde transport). B. Kymographs reveal both anterograde (slope down, left to right) and retrograde (slope down, right to left) DCV axonal transport in sLNv projections of PDF>Dilp2-GFP flies at ZT3 and ZT23. C. Flux ratios (anterograde/retrograde) at different times of the day. n values (number of hemibrains) for ZT 0, 3, 5, 8, 11, 14, 17, 20, 21, 22, 23 are 4, 10, 6, 6, 8, 6 ,8, 8,12, respectively. One-way ANOVA revealed significant difference ($P < 0.001$). Post-test analysis by Dunnett's multiple-comparison test is presented: ****$P < 0.0001$, ***$P < 0.001$, *$P < 0.05$.

**Figure 2. Dense-core vesicle flux and velocity in sLNv nerve terminal projections.**

A. Anterograde flux and B. Retrograde flux (vesicles/min) in PDF>Dilp2-GFP brains. n values for ZT 2-4, 8-10, 14-16, and 23 are 11,12,10, and 9, respectively. $P < 0.01$, one-way ANOVA. **$P < 0.01$, Dunnett's multiple-comparison post-test. C. Retrograde velocity of DCVs at ZT 3 and 23 in PDF>Dilp2-GFP brains (left, average of each brain; ZT3 n = 4, ZT 23 n = 4; right, average of all vesicles measured: ZT3 n = 49, ZT23 n = 51).

**Figure 3. Dependence of rhythmic capture on electrical activity, the PDFR and *per*.**

A. Ratios of anterograde to retrograde sLNv axonal DCV flux (A/R) at ZT3 and ZT23 in controls in which PDF>Dilp2-GFP and UAS-mCherry RNAi (*Bl*#35785) were crossed to account for expression of two UAS constructs (left two columns) and in experimental animals in which PDF>Dilp2-GFP and UAS-Kir2.1 flies were crossed (Kir, right two columns). In controls, n was 15 at ZT3 and 6 at ZT23. In Kir2.1, n = 14 for each time point. **P < 0.01 for control by unpaired t-test, while there was no significant difference for Kir (p = 0.62). B. Ratios of anterograde to retrograde DCV flux (A/R) at ZT3 and ZT23 in *w*; UAS-Dilp2-GFP; PDF-Gal4 controls (CON) and *han*; UAS-Dilp2-GFP; PDF-Gal4 PDFR null (*han*) sLNv axons. n $\geq$ 13 for CON; n > 20 for *han*. For both CON and *han*, ****P < 0.0001, unpaired t-test. C. Ratios of anterograde to retrograde DCV flux (A/R) 2 days after transition to constant darkness at CT3 and CT23 in *w*; UAS-Dilp2-GFP; PDF-Gal4 controls (CON), $Per^{01}$; *UAS-Dilp2-GFP; PDF-Gal4 PDFR* (80928) and $y^{1}Per^{01}w^{*}$; *UAS-Dilp2-GFP; PDF-Gal4* (80917) sLNv axons. n = 9 for CON; in 80917 and 80928 n = 6 for CT3 and n = 7 for CT23. **P < 0.01, unpaired t-test.

**Figure 4. A large releasable pool of DCVs is present at ZT1 in sLNv nerve terminals.**

A. Confocal images of the FAP signal in sLNv terminals following one-hour exposure to MG-Tcarb in normal HL3 saline (CON), MG-Tcarb in high $K^{+}$ HL3 saline (Hi K+), or with exposure to the membrane permeant MG analog MGnBu (500nM) in normal HL3 saline. Scale bar is 10 µm. B. Quantification of FAP-MG fluorescence in sLNv nerve terminals

exposed to MG-Tcarb in normal HL3 saline, MG-Tcarb in Hi K+ HL3 saline, or membrane permeable MGnBu in normal HL3 saline. ***$P < 0.001$, *$P < 0.05$. n = 10 for CON; n = 9 for Hi K+; n = 6 for MGnBu. One-way ANOVA revealed a significant difference ($P < 0.001$). Post-test analysis by Tukey's multiple-comparison test is presented: ***$P < 0.001$, *$P < 0.05$.

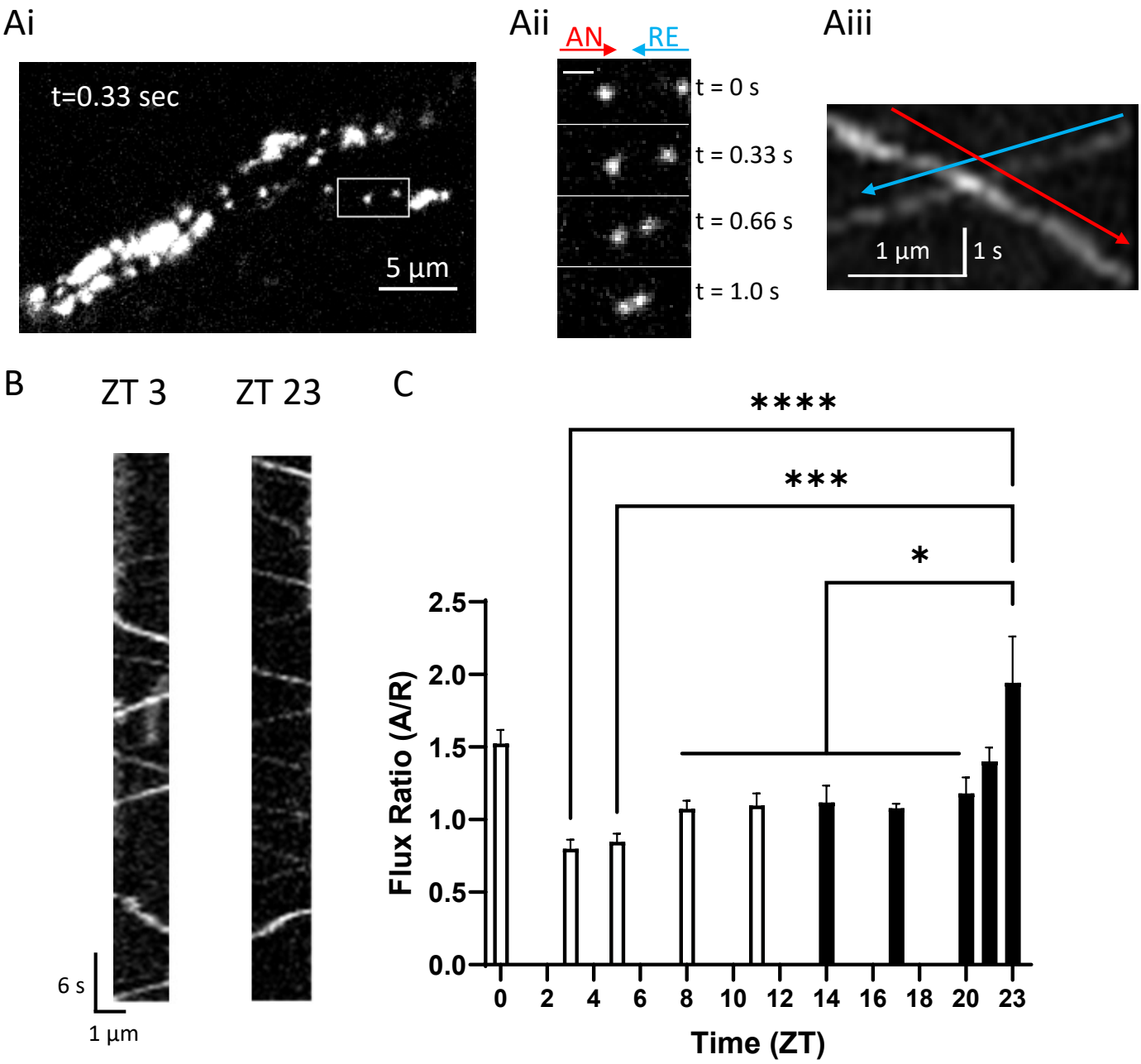
Ai
t=0.33 sec
5 µm
Aii
AN
RE
t = 0 s
t = 0.33 s
t = 0.66 s
t = 1.0 s
Aiii
1 µm
1 s
B
ZT 3
ZT 23
6 s
1 µm
C
****
***
*
Flux Ratio (A/R)
2.5
2.0
1.5
1.0
0.5
0.0
0
2
4
6
8
10
12
14
16
18
20
23
Time (ZT)

Figure 1

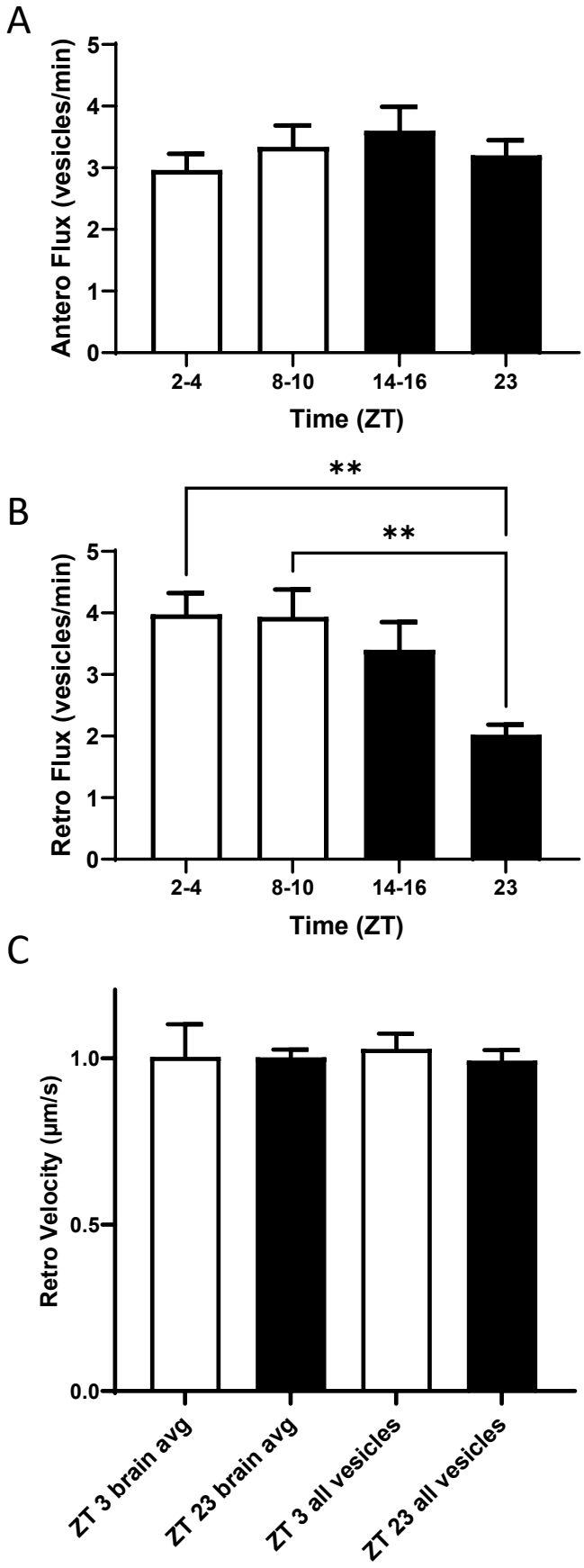
A
Antero Flux (vesicles/min)
0
1
2
3
4
5
2-4
8-10
14-16
23
Time (ZT)
B
**
**
Retro Flux (vesicles/min)
0
1
2
3
4
5
2-4
8-10
14-16
23
Time (ZT)
C
Retro Velocity (µm/s)
0.0
0.5
1.0
ZT 3 brain avg
ZT 23 brain avg
ZT 3 all vesicles
ZT 23 all vesicles

Figure 2

A

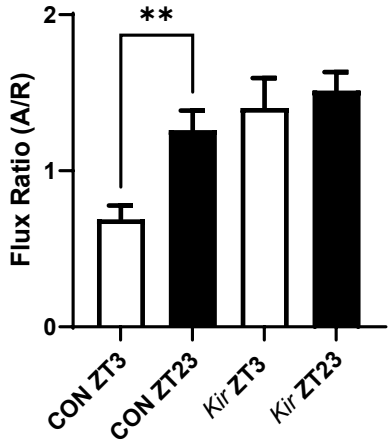
**
Flux Ratio (A/R)
2
1
0
CON ZT3
CON ZT23
Kir ZT3
Kir ZT23

B

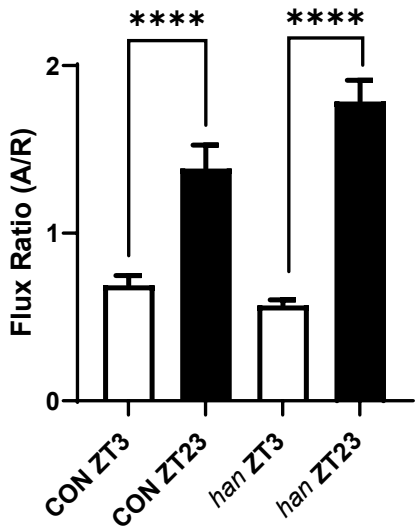
****
****
Flux Ratio (A/R)
2
1
0
CON ZT3
CON ZT23
han ZT3
han ZT23

C

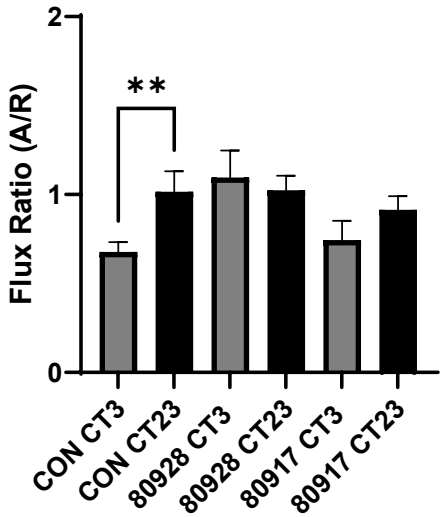
**
Flux Ratio (A/R)
2
1
0
CON CT3
CON CT23
80928 CT3
80928 CT23
80917 CT3
80917 CT23

Figure 3

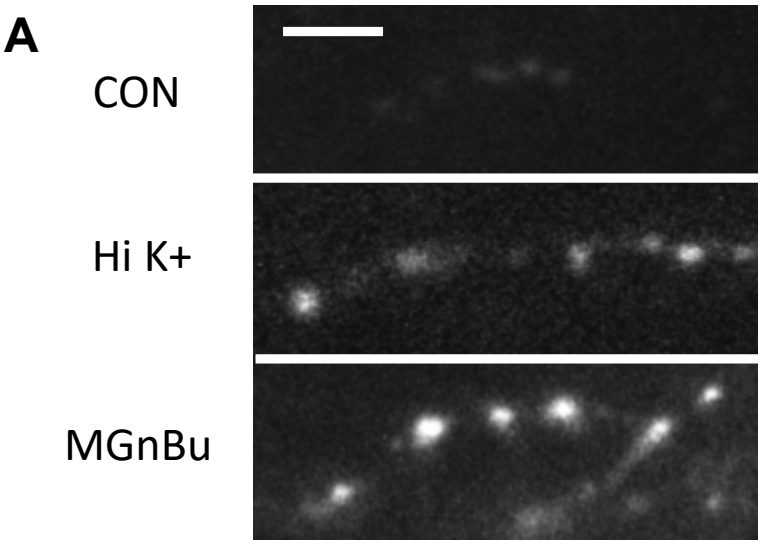
A
CON
Hi K+
MGnBu

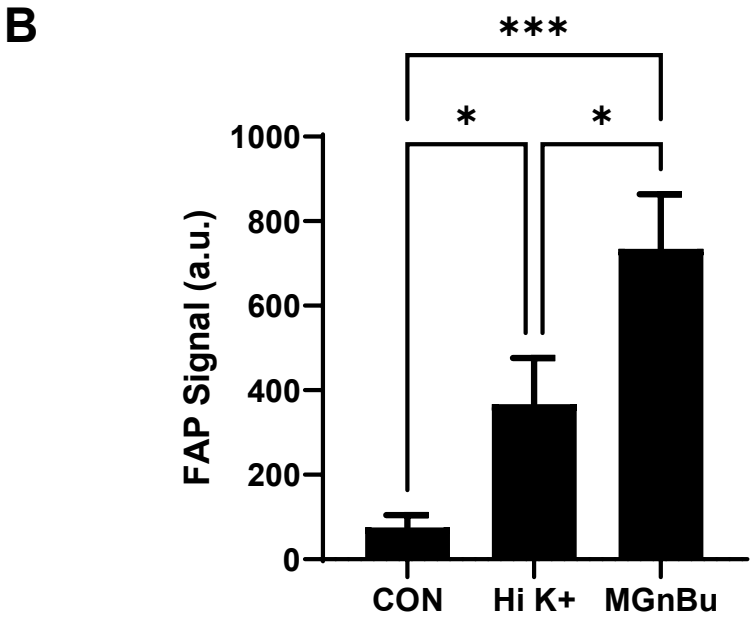
B
***
*
*
1000
800
600
400
200
0
FAP Signal (a.u.)
CON
Hi K+
MGnBu